Desalination and Water Treatment
www.deswater.com
doi: 10.1080/19443994.2013.871342

53 (2015) 3668–3680
March

Taylor & Francis
Taylor & Francis Group

Kinetics and thermodynamics of cationic dye adsorption onto dry and swollen hydrogels poly(acrylic acid-sodium acrylate-acrylamide) sodium humate

Tripti Singh, Reena Singhal*

Department of Plastic Technology, Harcourt Butler Technological Institute, Kanpur 208002, India
Emails: reena_singhal123@rediffmail.com; reenasinghal123@gmail.com

Received 27 May 2013; Accepted 26 November 2013

ABSTRACT

A novel superabsorbent hydrogel (SAH) composed of poly(acrylic acid-sodium acrylate-acrylamide)/sodium humate poly(AAc-SA-AM)/SH was synthesized and applied as adsorbent to adsorb crystal violet (CV) and methylene blue (MB) dye in its dry as well as swollen condition from the aqueous solutions. The swelling ratios of the synthesized SAHs were determined. The factors affecting adsorption capacity of the poly(AAc-SA-AM)/SH hydrogel, such as contact time, temperature, SH content (wt.%), and initial concentration of both dyes, were systematically investigated. The experimental data suggested that an appropriate addition of SH (2.40 wt.%) increases the swelling ratio as well as adsorption capacity of poly(AAc-SA-AM) hydrogel. The adsorption capacity was approximately equal for the dry (231 mg/g for CV and 270 mg/g for MB) and equilibrium SAHs (240 mg/g for CV and 278 mg/g for MB). The results also revealed that the swollen SAHs exhibited higher adsorption rate than the dry SAHs due to presence of functional anionic groups in its elongated state. The adsorption equilibrium data fitted very well to the Langmuir isotherm than the Freundlich isotherm. Thermodynamic parameters of adsorption were also calculated, and the negative change in ΔG° and ΔH° confirmed that the dye adsorption process was spontaneous and exothermic in nature. The kinetic studies showed that the adsorption phenomenon followed the pseudo-second-order kinetic model.

Keywords: Hydrogels; Dye adsorption; Adsorption kinetics; Thermodynamic parameter

1. Introduction

Nowadays, with the increased development of modern industries, various environmental contaminations associated with the coloring dyes existing in wastewaters of different industrial sectors such as printing, dying, cosmetics, papermaking, textile, food coloring, etc. has drawn much attention [1]. From environmental point of view, release of dyes into the water resources even in a small quantity has posed serious environmental problems to the aquatic life and food web (such as skin irritation, allergic dermatitis, and even cancer) [2–4]. Thus, colored effluents pose a challenge to the existing conventional methods for wastewater treatment. So, many conventional wastewater treatment methods that include electro-coagulation [5], oxidation or ozonation [6,7], membrane separation [8], coagulation and flocculation

*Corresponding author.

[9], and adsorption [10] have already been used for removing various dyes present in wastewater. Among these treatment methods, adsorption process exhibited particular advantages over the others due to its cheapness, effectiveness, simple design, flexibility, and insensitivity towards toxic pollutants and no production of harmful by-product to the treated water [11].

Superabsorbent hydrogels (SAHs) are three-dimensional chemically or physically cross-linked polymer networks, capable to swell in water, and increasing substantially their original weight while keeping their integrity. These SAHs are used in many applications including hygiene products (disposable diapers, surgical pads, and sanitary napkins, etc) [12] and in medicine used for the drug-delivery systems [13,14]. Besides, to health care products, they are applied in soil for agricultural and horticultural programs [15], sealing material, drilling fluid additives, water-blocking tapes, gel actuators [16], anti-redecomposition agents for detergent formulations and communication cables.

SAHs possess ionic functional groups such as amine, hydroxyl carboxylic acid, and sulfonic acid groups; they may adsorb and trap cationic dyes such as MB [17] or metal ions [18,19] from wastewater. Thus, a considerable attention has been given to SAHs with chelating functional groups for the adsorption and separation of dyes from dyes contaminated water.

Most of the SAHs used in practice are primarily formed of pure synthetic polymers with high production cost, low stability, as well as poor environment friendly characteristics. So, to overcome these drawbacks, the development of SAHs, with the introduction of natural raw materials, which are low in cost, non-toxic, biodegradable in nature and renewable such as humic acid or humates has been focused upon. Humic acid, a principal component of humic substances, is found in many places in nature. It consists of multifunctional aromatic components and aliphatic constituents and has large number of functional hydrophilic groups (such as carboxylates and phenolic hydroxyls) [20]. Existence of these carboxylate and phenolate groups helps sodium humate to form complexes/chelates with dye molecules.

Hizal and Apak [21] observed that clay mineral, in the presence of humic acid, act more like a chelating agent for adsorption of metal ion than a simple ion exchanger and so in the presence of humic acid the stability of surface complexes was more in comparison to binary metal ion complexes. Solpan et al. [22] have prepared poly(acrylamide-co-acrylic acid (poly (AAm-co-AAc)) hydrogels by irradiating with gamma radiation and applied it for the adsorption of cationic dyes such as Safranine-O (SO) and Magenta (M).

Although, there are many investigations on the adsorption of dyes onto the SAHs in their dry state, nevertheless, as to the best of our knowledge, none of these reports evaluated the adsorption kinetics and thermodynamic parameters of adsorption onto SAHs already swollen to equilibrium. The SAHs of the domestic waste, in contact with textile exist in its dry or equilibrium swollen state in waste.

In the present study, a novel biodegradable multifunctional SAHs composed of acrylic acid (AAc), sodium acrylate, and acrylamide monomers and modified with sodium humate was synthesized; as a combination of natural and synthetic polymers. The synthesized SAHs (in dry as well as equilibrium swollen state) were applied for the adsorption of crystal violet (CV) and methylene blue (MB) dye molecules. The effects of SH content, contact time, temperature and initial CV, and MB dye molecules concentration on the adsorption capacity were investigated. Kinetic data and models fit to equilibrium adsorption isotherm for the adsorption process were evaluated here to understand the adsorption mechanism to validate the usefulness of this novel hydrogel in the field of wastewater treatment. Thermodynamic parameters for the adsorption process of CV and MB dye molecules were also investigated. We also investigated the simultaneous adsorption of above two dyes from their aqueous mixture. The desorption capacity as well as the reusability of this solid adsorbent poly(AAc-SA-AM)/SH were assessed based on four consecutive adsorption–desorption cycles.

2. Experimental

2.1. Materials

AAc (analytical grade), acrylamide (AM, analytical grade), ammonium per sulphate (APS, analytical grade), sodium hydroxide (NaOH, analytical grade), and N,N-methylene bisacrylamide (NMBA, analytical grade), were purchased from CDH New Delhi, India. Methanol (analytical grade), CV, and MB dyes (spectroscopic grade) were purchased from Qualikems, New Delhi. AM was recrystallized from methanol before use. Sodium humate (SH, analytical grade), (supplied from Aldrich) was used as received. Double distilled water was used throughout the experiments.

2.2. Synthesis of poly(AAc-SA-AM)/SH SAHs

Synthesis of poly(AAc-SA-AM)/SH SAHs can be described as AM (5 g) was dissolved in 10 ml distilled water. Seven grams of AAc were neutralized

with NaOH solution. Then, AAc/SA was added to AM solution under constant stirring and after that the reaction mixture solution was taken in a 250 ml-three-neck round bottom flask. The cross-linker NMBA (0.21 wt.% of total monomer) was added to the reaction mixture solution and then appropriate amount of SH was dispersed into mixed solution. Then, the reaction mixture solution was stirred with nitrogen for 30 min, and then the mixed solution was heated at 60˚C in a thermostat oil bath gradually and after that the APS (0.40 wt.% of total monomer) was introduced. The reaction solution was stirred vigorously maintaining the nitrogen atmosphere until the gel was formed. After complete polymerization, the reaction product was removed, cut into small pieces and then washed with methanol followed by water, and then dried in an oven at 60˚C.

The actual feed compositions for the synthesis of poly(AAc-SA-AM)/SH SAHs are provided in Table 1.

2.3. Fourier transforms infrared spectroscopy (FT-IR) studies

The FT-IR spectra of the synthesized poly(AAc-SA-AM)/SH SAHs and after swelling in CV and MB solutions were recorded with Perkin Elmer Spectrophotometer using solid pellet potassium bromide (KBr) after completly drying the sample at 60˚C to constant weight.

2.4. Scanning electron microscopy

The surface morphology of poly(AAc-SA-AM)/SH (SH_4) hydrogel before and after dye adsorption was examined under the scanning electron microscope (SEM). Dried SAHs were coated with a thin layer of pure gold in S150 Sputer Coater, and imaged with a SEM (LEO Electron Microscopy Ltd. England).

Table 1
The feed compositions for synthesis of various poly(AAc-SA-AM)/SH SAHs

Sample designation	AAc (wt%)	SA (wt%)	AM (wt%)	SH (wt%)
H_0	12.50	37.50	50.00	00.00
H_1	14.36	43.10	41.05	1.47
H_2	14.29	42.89	40.84	1.96
H_3	14.22	42.68	40.65	2.40
H_4	14.15	42.47	40.45	2.91
H_5	14.09	42.27	40.25	3.38

Note: Other conditions: NMBA, 0.21 wt%; APS, 0.40 wt%; distilled water, 30 ml; temperature 60˚C.

2.5. Equilibrium swelling studies

The completely dried preweighed SAHs samples were placed in 1,000 ml distilled water (sink condition) at the room temperature 30.0 ± 5.0˚C. Then, the swollen gel samples were taken out at regular time intervals and their surface were quickly blotted free of water with the help of filter paper. After that it was weighed and then placed in same bath. This mass measurement was continued till the attainment of the equilibrium swelling.

The equilibrium swelling (S_{eq}) was determined following the conventional gravimetric method by applying the following equations:

$$S_{eq}(g/g) = \frac{\text{Equilibrium swollen weight} - \text{dry weight}}{\text{dry weight}} \quad (1)$$

2.6. Measurement of CV and MB dye molecules adsorption

To study the adsorption of CV and MB dye molecules, 50 mg of dry hydrogel was introduced in 100 ml of CV and MB dye solution and was left in their solutions at different constant temperatures (±0.5˚C) for 48 h. Then, the samples were withdrawn at various predetermined time intervals (1, 2, 3, 4, 5, 6, 7, 8, 9, 10, 11, 12, 24, and 48 h), and 2 ml of solution was sampled to analyze CV and MB dye molecules content left in solution by UV–vis spectroscopy. The dye content in supernatant solution was evaluated at characteristic wavelength 665 nm for CV and 617 nm for MB by UV–visible spectrophotometer. The various absorbance values at λ_{max} were converted to their concentration with the help of predetermined calibration curves of each dye.

The analysis of adsorption capacities for the poly (AAc-SA-AM)/SH SAHs for CV and MB dye were performed through the following equation:

$$q_e = \frac{C_o - C_e}{m} \times V \quad (2)$$

where q_e is the amount of CV/MB dye molecules adsorbed at equilibrium, C_o is the initial concentration of CV/MB dye molecules, C_e is the equilibrium concentration of CV/MB dye molecules, V is the volume of the CV/MB dye molecules, and m is the mass of hydrogel sample.

Adsorption of CV and MB dye molecules onto poly(AAc-SA-AM)/SH SAHs done in both dry as well as equilibrium swollen condition state. To study the adsorption in dry state the above given process

was applied. To investigate the adsorption in equilibrium swollen state, firstly the SAHs was swollen to its equilibrium state and after achieving the equilibrium swelling, the equilibrium swollen sample was taken out and the excess water was drained out. These swollen samples were used for the dye adsorption study onto equilibrium swollen sample.

In order to evaluate the influence of temperature on adsorption capacity for CV/MB dye molecules, isotherms were established at 30, 45, and 60°C.

For the kinetic study adsorption experiments were conducted as follows: pre-weighed SAHs samples were suspended in 100 ml solution containing 350 mg/L of CV/MB dye molecules. Then, the sealed flasks were put in a shaker bath at 30 ± 0.5°C. The flasks were then taken out at different times for the analysis of CV/MB dye molecules. The rate of CV/MB dye molecules adsorption was evaluated from the amount of CV/MB dye molecules adsorbed at different times.

2.7. Desorption and regeneration

Elution of CV/MB dye molecules from the poly (AAc-SA-AM)/SH hydrogel was carried out in 500 ml distilled water for 48 h at temperature 30 ± 0.5°C. The hydrogel-adsorbed CV/MB dye molecules was placed in the distilled water and stirred with a magnetic stirrer at room temperature. The SAHs was washed several times with distilled water and followed by methanol, and then dried at 60°C for 48 h. The obtained regenerated SAHs hydrogel was employed for another adsorption. The final CV/MB dye concentration in the aqueous phase was determined by UV–vis spectroscopy. Desorption ratio was calculated from the amount of CV/MB dye ions adsorbed on the polymer surface and final CV/MB dye molecules concentration in the elution medium.

Desorption ratio was calculated using the following expression:

$$\text{Desorption } \% = \frac{\text{Amount of MB/CV dye desorbed to the elution medium}}{\text{Amount of MB/CV dye adsorbed on the superabsorbent hydrogel}} \times 100 \quad (3)$$

In order to determine the reusability of the SAHs consecutive adsorption desorption cycle was repeated for the five times of the same sample.

3. Result and discussion

3.1. Fourier transforms infrared spectroscopy (FT-IR) studies

The FT-IR technique was applied for the characterization of poly(AAc-SA-AM)/SH SAHs before and after the adsorption of dye molecules. The FT-IR spectra of representative sample poly(AAc-SA-AM)/SH SAHs before and after CV and MB dye adsorption were investigated and displayed in Fig. 1. Few facts are readily apparent in the figure. A broad band corresponding to –NH stretching vibrations of $–NH_2$ functional group (AM) and overlapping absorption bands of O–H functional group due to formed hydrogen bonding and AAc existing at 3,447 cm^{-1} was broadened after the dye adsorption and appeared at 3,441 and 3,436 cm^{-1} for CV and MB, respectively, because of combined interaction of CV and MB dye molecules with the –OH functional group. The characteristic band at 1,715 cm^{-1} assigned to C=O group of carboxyl functional group after adsorption of CV and MB dye molecules appeared at 1,694 and 1,690 cm^{-1}, respectively. An absorption band present at 1,560 cm^{-1} ascribed due to symmetric stretching was now shifted at 1,522 and 1,520 cm^{-1} for CV and MB dye as well as an absorption band at 1,400 cm^{-1}; because of asymmetric stretching, the carboxylate groups now appeared at 1,456 and 1,452 cm^{-1} CV and MB dye, respectively. On the basis of FT-IR spectra observation it can be concluded that the CV and MB dye adsorption onto the poly(AAc-SA-AM)/SH SAHs surface mainly occurred through chelation and ion exchange mechanism formed between positively charged CV and MB dye molecules and carboxylates as well as phenolic hydroxylics.

3.2. Scanning electron microscopy

The SEM images of poly(AAc-SA-AM)/SH SAHs (H_3) before and after the dye adsorption are shown in Fig. 2. It can be observed from Fig. 2(a) that the structure of H_3 SAHs prior to dye adsorption is highly porous. Fig. 2(b) and (c) show the SEM of above SAHs after 48 h of CV and MB dye adsorption. It is obvious from Fig. 2(b) and (c) that CV and MB dye adsorption

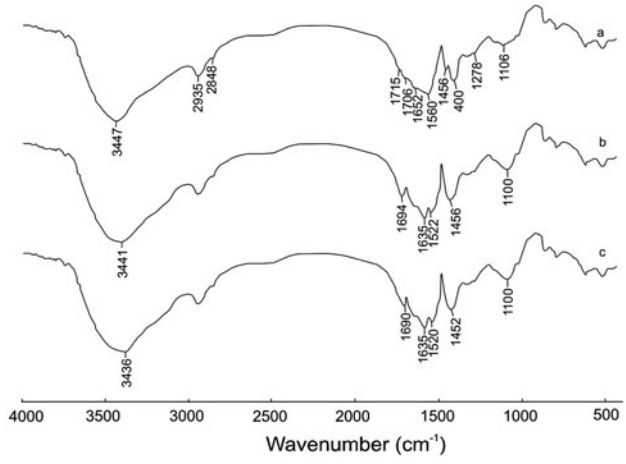

Fig. 1. FT-IR spectra of (a) poly(AAc-SA-AM)/SH (H_3) SAHs, (b) poly(AAc-SA-AM)/SH (H_3) SAHs after swelling in CV dye solution, and (c) poly(AAc-SA-AM)/SH (H_3) SAHs after swelling in MB dye solution.

blocks the open pores of SAHs. The adsorption of CV and MB dye onto the H_3 SAHs, leads to the formation of a smooth and nonporous surface morphology, which is because of the newly formed layer of dye molecules on the SAHs surface. These evidences clearly suggest that dye molecules have a prominent influence on the structure of poly(AAc-SA-AM)/SH SAHs surface by sealing the pores.

3.3. Effect of content of sodium humate on equilibrium swelling

The relationship between SH content variation and equilibrium swelling in distilled water, CV and MB dye is displayed in Fig. 3. It can be easily seen from Fig. 3 that initially, the equilibrium swelling in distilled water was increased slightly from 378 to 536 g g^{-1} for the SAHs H_1 to H_2 with SH concentration 1.40 to 1.96 wt.%. After that the equilibrium swelling ratio increased drastically from 536 to 747 g g^{-1} for H_2 to H_3 SAHs that have 1.96 to 2.40 wt.% SH content in the feed. On further increasing the content of SH from 2.40 to 3.38 wt.%, the equilibrium swelling shows sharp decrease for H_3 to H_5 hydrogels. The SAHs, H_3 exhibits maximum equilibrium swelling of 747 g g^{-1}. The increment in equilibrium swelling can be explained as, SH; a complex organic macromolecule, consists free and bound phenolic –OH groups, oxygen, and nitrogen

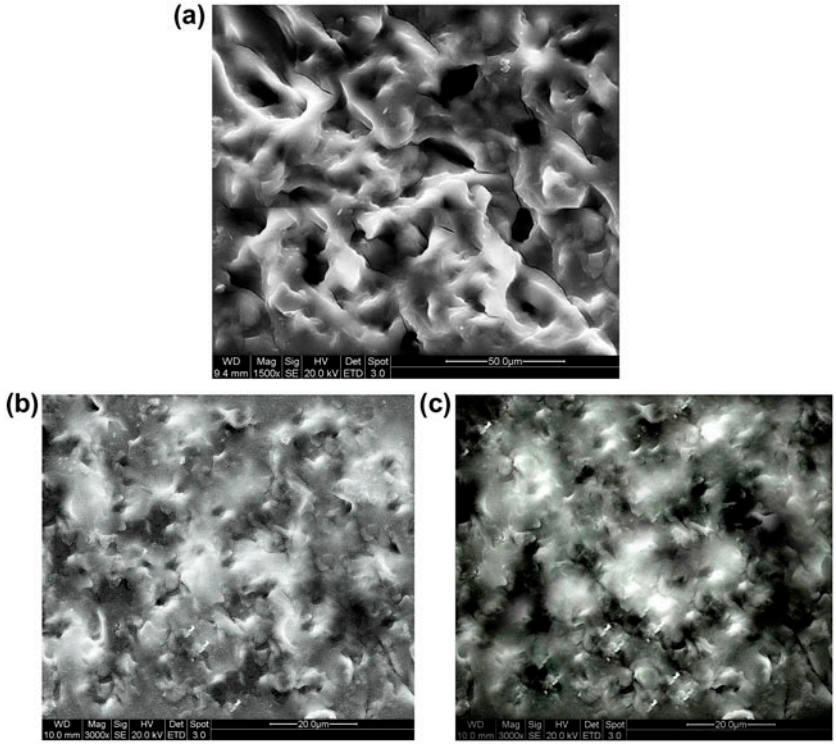

Fig. 2. (a) SEM of poly(AAc-SA-AM)/SH SAHs (H_3) superabsorbent hydrogel, (b) SEM of poly(AAc-SA-AM)/SH SAHs (H_3) superabsorbent hydrogel after swelling in CV dye solution, and (c) SEM of poly(AAc-SA-AM)/SH SAHs (H_3) superabsorbent hydrogel after swelling in MB dye solution.

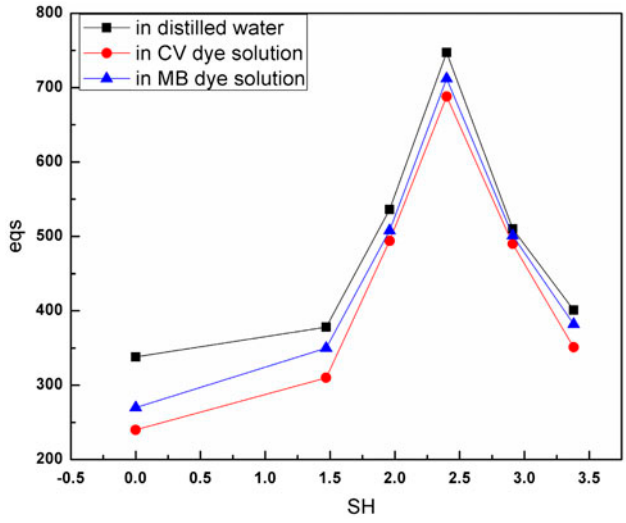

Fig. 3. Effect of SH concentration (wt%) on equilibrium swelling of poly(AAc-SA-AM)/SH SAHs.

acting as bridge unit, quinine structure, –COOH and $–NH_2$ groups placed on the aromatic ring [22,23]. The species and the number of hydrophilic groups present onto the poly(AAc-SA-AM)/SH SAHs network were much more, and they react with AAc and AM during the polymerization process. The introduction of irregular SH into SAHs poly(AAc-SA-AM) polymeric network decreases the effective cross-linking density that causes increased equilibrium swelling with increasing SH content. However, as the SH content increases above 2.43 wt.%, the decrease in equilibrium swelling may be because of the fact that excessive SH particles only act as a filler and so the amount of hydrophilic groups present onto the polymeric backbone decreased on increasing the SH content [24]. Thus, formation of an efficient adsorbent three-dimensional structures became difficult and the solubility of SAHs increased. Similar type of observation has been reported by Liu et al. [25] for SAHs formed of chitosan-g-poly(acrylic acid)/sodium humate having various concentration of SH. They find out that equilibrium swellling increases from 0 to 10% SH content and after that decreases and SAHs having 10 wt.% SH show the equilibrium swelling of 183 g g^{-1}.

3.4. Adsorption mechanism

Many investigations have been worked out on the binding of dyes to polyelectrolytes. Generally, two possible mechanisms for cationic dye adsorption can be considered. First one is the interaction among the positively charged cationic dye molecules and negative active binding site onto the adsorbent surface occurring mainly because of electrostatic forces [26]. These interactions held at the adsorbate/adsorbent interface. The adsorption takes place through the phenolic hydroxyls and carboxylates functional groups as these groups

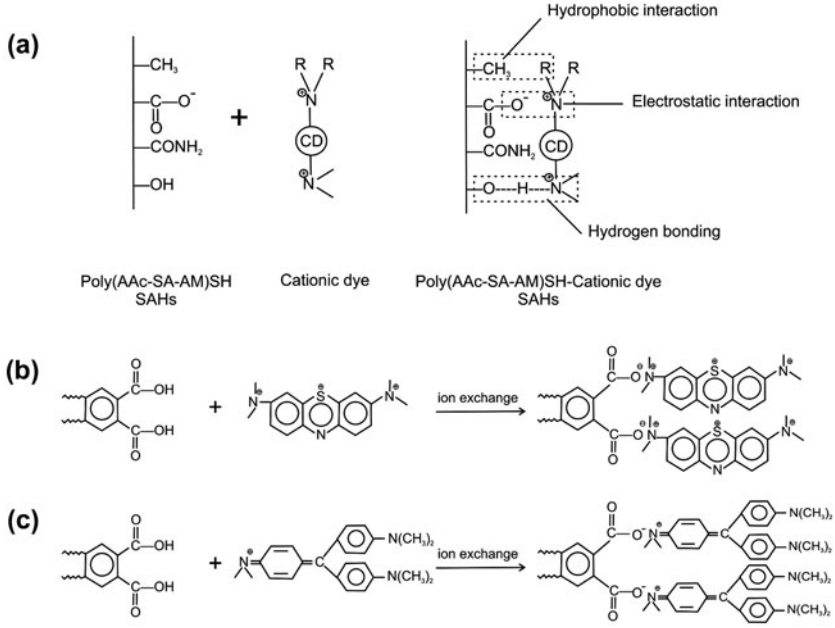

Fig. 4. (a) Possible complexation process between poly(AAc-SA-AM)/SH SAHs and cationic dye, (b) Adsorption mechanisms of MB adsorption onto poly(AAc-SA-AM)/SH SAHs, and (c) Adsorption mechanisms of CV adsorption onto poly(AAc-SA-AM)/SH SAHs.

have high affinities towards cationic dyes [27], so an ionic complex formed between the positively charged functional groups of dyes and negatively charged functional groups of SAHs. Then, the other type of interactions are hydrophobic and hydrogen bonding. Hydrophobic interaction is an aqueous solutions interaction which in this case involves the methane and methyl groups and aromatic rings existing on the SAHs. Hydrogen bonding may specifically involve the reactive –OH and –COOH groups present on SAHs polymer chains and the amine groups of cationic dye (Fig. 4).

For the dry samples, the adsorption occurs with the swelling. In the case of swollen sample the adsorption takes place after the swelling. As in case of dry SAHs due to simultaneous swelling and adsorption, all the anionic functional groups are not available at the beginning so initially the dye molecules are adsorbed by the anionic functional groups present on the surface of the SAHs. As the swelling proceeds, more anionic functional groups become available for interaction. For the equilibrium swollen sample the dye molecules replaced the already adsorbed water molecules. In the equilibrium swollen state, the polymeric chains are in its fully elongated confirmations and so all the anionic functional groups are accessible from the initial stage for the adsorption of dye molecules. Thus, the equilibrium swollen sample shows slightly higher adsorption capacity as well as faster rate of adsorption.

The findings of IR investigations (i.e. shift in characteristic asymmetric stretching band of carboxylate and C=O group of carboxyl group) also confirmed the COO^- and –COOH functional group involvement in the adsorption process.

3.5. Effect of contact time on adsorption of CV/MB dye molecules

In order to investigate the influence of contact time on the adsorption of CV/MB dye molecules onto poly (AAc-SA-AM)/SH SAHs from aqueous solution, the SAHs samples in dry as well as equilibrium swollen state were equilibrated with adsorbate solution for various predetermined period, as shown in Fig. 5. As clear from Fig. 5, it can be observed that the adsorption capacity of hydrogel for CV/MB dye both molecules rapidly increased with the increase in contact time of adsorption because initially adsorption sites were void and dye molecules easily interacted with these sites.

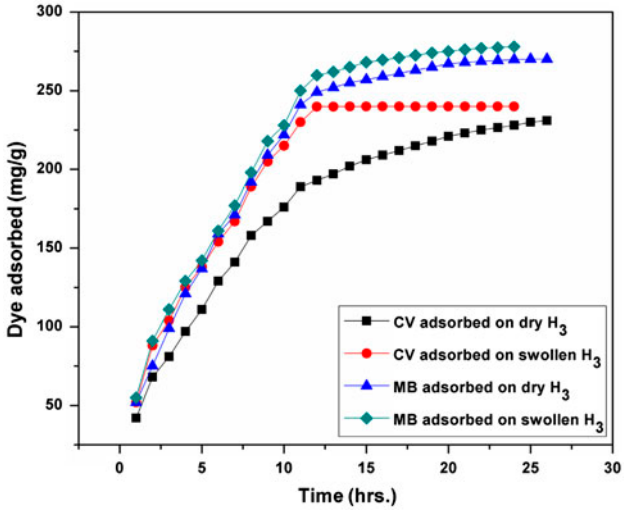

Fig. 5. Effect of contact time on the adsorption of CV and MB dye in dry as well as equilibrium swollen condition initial ion concentration, 350 mg/L; temperature 30 ± 0.5°C; hydrogel content, 50 mg.

It is also observed from Fig. 5 as well as Table 2 that adsorption capacity of the SAHs is approximately equal for the dry and equilibrium swollen SAHs. Rate of adsorption for both dyes was faster for the equilibrium swollen SAHs sample than the dry SAHs. For the dry SAHs the swelling and adsorption process occur simultaneously. So, in dry state all the active

Table 2
Estimated adsorption kinetic parameters for the adsorption of CV and MB dye onto SAHs H_3 in aqueous solutions

		Pseudo-first-order model				Pseudo-second-order model			
Sample designation	Dye	q_e exp. (mg/g)	q_{1e} cal. (mg/g) Linear/ non linear	$k_1 \times 10^3$ (min) Linear/ non linear	R^2 Linear/ non linear	q_e exp. (mg/g) Linear/ non linear	q_{2e} cal. (mg/g) Linear/ non linear	$k_2 \times 10^4$ (g/mg min) Linear/non linear	R^2 Linear/ non linear
SAHs H_3 in dry state	CV	231.00	323.59	20.49	0.97	231.00	294.00	4.80	0.99
	MB	270.00	562.34	29.93	0.94	270.00	344.00	4.47	0.98
SAHs H_3 in swollen state	CV	240.00	301.99	25.33	0.90	240.00	303.00	6.52	0.97
	MB	278.00	275.42	13.81	0.98	278.00	357.00	4.30	0.99

functional groups are unavailable at the initial state for adsorption but with the progress in swelling their availability for adsorption becomes more due to increased elongation of polymeric chains. Therefore, because of presence of more interaction site to dye molecules the swollen samples exhibit higher adsorption rate.

3.6. Effect of SH content on adsorption of CV/MB dye molecules

Effect of SH content on adsorption capacity of poly (AAc-SA-AM)/SH SAHs for CV (initial concentration 350 mg/L; temperature 303.15 K) and) and MB (initial concentration 350 mg/L; temperature 303.15 K) dye molecules has been shown in Fig. 6. It can be examined from the figure that in the same conditions the adsorption amount of poly(AAc-SA-AM)/SH SAHs with various concentration of SH are different. Poly(AAc-SA-AM)/SH SAHs show higher adsorption capacity than that of poly(AAc-SA-AM) SAHs. It can also be observed that adsorption amount of poly(AAc-SA-AM)/SH SAHs increases for CV and MB both dye molecules when the content of SH was less than 2.4 wt.%. SH has many functional groups that have capability to react with AAc, SA, and AM during polymerization process and improves the polymeric network; thus enhanced the adsorption capability to a certain extent. However, on further increasing the SH amount above 2.4 wt.% resulted in a decrease of adsorption efficiency. This phenomenon can be explained as there are lots of –OH groups present on the surface of SH molecule, and thus SH particles can function as cross-linking points in the polymeric network. Therefore, higher SH content could form more cross-link points and so the elasticity of the molecular polymeric network decreased, which decreases the adsorption amount of the SAHs. Additionally, at higher SH concentration the amount of hydrophilic groups existing on the polymeric backbone decreased which results in difficulty of the formation of efficient three-dimensional structures of adsorbent and thus decreased the adsorption efficiency.

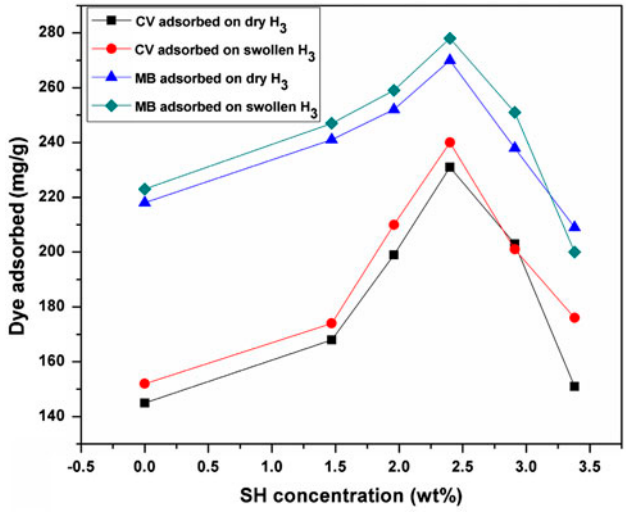

Fig. 6. Effect of SH concentration on the adsorption of CV and MB dye onto poly(AAc-SA-AM)/SH SAHs contact time, 48 h; initial ion concentration, 350 mg/L; temperature 30 ± 0.5°C; hydrogel content, 50 mg.

3.7. Adsorption kinetics

Kinetic studies are beneficial to understand the mechanism of dye molecules adsorption process as well as to judge the performance of the adsorbents applied for dye adsorption.

Lagergren pseudo-first-order [28] and Ho and McKay's pseudo-second-order kinetics model [29], the two widely used models applied for the solid–liquid adsorption. These two models were shown by the following equations, respectively.

$$\log(q_{1e} - q_t) = \log q_{1e} - k_f t/2.303 \quad (4)$$

$$t/q_t = 1/(k_s q_{2e}^2) + t/q_{2e} \quad (5)$$

where q_{1e}, q_{2e}, and q_t (mg/g) represent the amount of dye molecules adsorbed per unit mass of SAHs at equilibrium and at any time t, respectively. The parameter k_f (min^{-1}) is the rate constant for the pseudo-first-order model, and k_s (g/(mg min)) is the rate constant for the pseudo-second-order model. The parameters q_{1e} and k_f may be calculated from the intercept and slope of the plot of log ($q_{1e} - q_t$) vs. t. In the same manner, the intercept and slope of the plot of t/q_t against t gives the values of k_s and q_{2e}. The initial adsorption rate r_{id} (mg/g/min) is evaluated using the equation $r_{id} = k_s\, q_{2e}^2$. The experimental data for the adsorption of CV and MB dye molecules in both dry as well as equilibrium swollen state are analyzed by the above two kinetic models and the parameters calculated from above given equations together with correlation coefficients are tabulated in Table 2.

It was examined from Table 2 that the correlation coefficients (R^2) of the CV and MB dye adsorption for the pseudo-first-order kinetic model were obtained between 0.90 and 0.98 (with the large differences between the calculated q_{1e} values and experimental q_e values ($q_{e,exp}$)), which reveals that pseudo-first-order kinetic model did not fit well for the adsorption

processes. It can also be observed from Table 2 that the correlation coefficients (R^2) for the pseudo-second-order kinetic model had extremely high values at around 0.98 (having q_{2e} values in good agreement with the experimental data ($q_{e,\exp}$) values), which showed that pseudo-second-order kinetic model can describe well the adsorption kinetics of CV and MB dye onto poly(AAc-SA-AM)/SH SAHs for the whole adsorption process. Thus, the results obtained suggest that the pseudo-second-order adsorption kinetic model well describe the adsorption process, and so implies that adsorption rates of both dyes onto the poly(AAc-SA-AM)/SH SAHs adsorbents are probably controlled by the chemical process.

3.8. Effect of initial concentration of CV/MB dye molecules on adsorption capacity

Adsorption capacity of the poly(AAc-SA-AM)/SH SAHs in dry as well as in swollen to equilibrium condition, for the CV and MB dye molecules as a function of different initial dye concentrations ranging from 100 to 350 mg/L was given in Fig. 7. As clearly seen from Fig. 7, the amount of dye molecules adsorbed on to the poly(AAc-SA-AM)/SH SAHs increased with increase in initial concentration of dye solution if the amount of adsorbent was kept unchanged. This can be explained as, when the initial dye concentration was low, the amount of the anionic functional groups in the SAHs is more in comparison

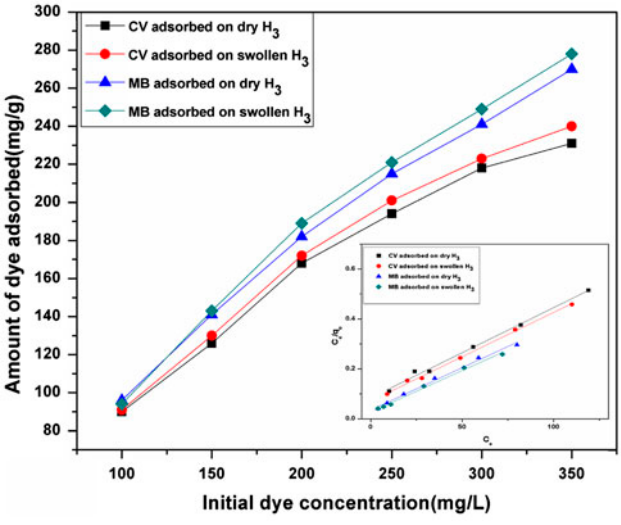

Fig. 7. Variation in the adsorption capacity as function of initial CV and MB dye concentration using poly(AAc-SA-AM)/SH SAHs in dry as well as equilibrium swollen condition. Inset figure (Langmuir adsorption isotherm for adsorption of CV and MB dye in dry as well as equilibrium swollen condition).

to amount of dye molecules. In addition to this, increase in the driving force of the concentration gradient at the high initial dye concentration. The initial dye concentration provides the driving force to conquer the resistance to the mass transfer of dye molecules between liquid and solid phases [30]. At a fixed adsorbent dose, the adsorption capacity of the adsorbent increased with increasing concentration of dye solution, on the other hand the percentage of adsorption decreased or for high initial dye concentration the residual concentration of dye molecules will be high. At the low concentration of dye molecules the ratio of initial number of dye molecules to the available active binding sites is low and due to that the fractional adsorption becomes independent of initial dye concentration. Then, after obtaining a maximum at 350 mg/L, the adsorption capacity levels off. From these values the maximum adsorption capacities for H_3 SAHs were found to be 231 and 240 mg/g/L for CV (in dry and equilibrium swollen sample, respectively) and 270 and 278 mg/g/L for MB (in dry and equilibrium swollen sample, respectively). After a certain initial concentration of dye molecules, dye molecules concentration exceeds the concentration of the anionic functional groups present on the SAHs surface, so the number of available active sites becomes lesser. Due to this all the dye molecules cannot be adsorbed and the SAHs become saturated after adsorbing a fixed amount of the dye molecules and subsequently the adsorption of dye depends on the initial concentration.

3.9. Equilibrium point adsorption

The equilibrium adsorption isotherm is fundamental to describe how solutes or adsorbate interact with adsorbent and so, equilibrium adsorption isotherms are critical in optimizing the application of adsorbent. The adsorption experimental data are generally interpreted using the Langmuir and Freundlich isotherm models.

The Langmuir adsorption isotherm model is derived by assuming a structurally homogeneous adsorbent surface, where all the binding sites are identical and with equal adsorption activation energy for the adsorption of each molecule onto the adsorbent surface energetically equivalent. The Langmuir adsorption model is applied for the fitting of experimental data of a monolayer and/or chemical adsorption. The adsorption data of CV/MB dye molecules adsorption onto poly(AAc-SA-AM) SAHs and poly(AAc-SA-AM)/SH SAHs have been interpreted using this model. It provides a quantitative relationship between the concentration of CV/MB dye molecules in the solution and the amount of CV/MB dye molecules adsorbed

onto solid phase when the existing two phases are at equilibrium. The Langmuir adsorption isotherm equation may be represented as [31,32]:

$$\frac{C_e}{q_e} = \frac{1}{K_e q_{\max}} + \frac{C_e}{q_{\max}} \quad (6)$$

The Freundlich model is used to describe a heterogeneous surface system which is characterized by a heterogeneity factor of $1/n$. This model is described by reversible adsorption and it is not restricted to the production of the monolayer. The Freundlich model in linear form may be shown as follows [33]:

$$\log(q_e) = \frac{1}{n}\log(C_e) + \log K_f \quad (7)$$

where K_e is the adsorption equilibrium constant (L/mg)) and $q_{\max}$ is maximum capacity of adsorption (mg/g), and C_e is the equilibrium concentration of the dye in the solution (mg/L), q_e is the adsorption capacity at equilibrium mg/g. $1/n$ (dimensionless) and K_f (L/g) are the Freundlich constants and related to the degree of heterogeneity and adsorption capacity, respectively. The Langmuir and Freundlich constants and linear regression coefficients were evaluated by plotting the linear plots of C_e/q_e vs. C_e and log (q_e) vs. log (C_e), respectively.

The isotherm constant parameters and linear regression coefficients obtained from Langmuir and Freundlich adsorption isotherm equations mentioned above are tabulated in Table 3.

It can be observed from the fit of the experimental data for CV/MB dye molecules adsorption that the values of linear regression coefficients for Langmuir model were higher than those of Freundlich model during the whole concentration investigated. So, the linearity obtained from Langmuir adsorption isotherm model correctly fitted the equilibrium data. The plots of Langmuir adsorption isotherm of CV and MB dye molecules (onto dry and equilibrium swollen SAHs sample) are shown in inset Fig. 7. The $q_{\max}$ values of the SAHs evaluated by Langmuir equation were quite consistent with the experimental one (Table 3). The higher values of correlation coefficient (R^2 value found in the range of 0.9813–0.9985 and 0.9891–0.9997 for Pb^{2+} ions and Fe^{2+} ions, respectively) signifies the applicability of Langmuir isotherm model and suggest the favorable and monolayer adsorption process. Therefore, it can be concluded that the adsorption process for CV and MB dye molecules can be satisfactorily described by Langmuir adsorption isotherm.

3.10. Thermodynamic parameters of adsorption

The equilibrium constants obtained from Langmuir adsorption equation at 30, 45, and 60°C were used to calculate the various thermodynamic activation parameters such as Gibbs free energy change (ΔG), standard enthalpy change (ΔH), as well as standard entropy change (ΔS). These thermodynamic parameters are the actual indicators of an adsorption process for its practical application. Depending on the values of these parameters, spontaneity of any adsorption process can be determined. In the present case, these parameters were calculated for the H_3 SAHs. The change in Gibbs free energy of any reaction can be expressed as follows [34]:

$$\Delta G = \Delta G^\circ + RT \ln K_e \quad (8)$$

When the adsorption acquires the equilibrium condition, then ΔG becomes zero, and so ΔG° will be equal to $-RT \ln K_e$, here K_e signifies the equilibrium constant, R represents the universal gas constant (8.314 J mol^{-1} K^{-1}), and T defines the temperature in Kelvin.

Temperature dependence of any reaction for the Gibbs free energy change can be given by the following equation [35]:

$$d(\Delta G^\circ/T) = -\Delta H^\circ/T^2 dT \quad (9)$$

$$\ln K_e = -(\Delta H^\circ/R)(1/T) + \Delta S^\circ/R \quad (10)$$

Table 3
Estimated adsorption isotherm parameters for the adsorption of CV and MB dye onto SAHs H_3 in aqueous solutions

		Langmuir model				Freundlich model		
Sample designation	Dye	q_e (mg/g)	$q_{\max}$ (mg/g)	$K_e \times 10^2$ (L/mg)	R^2	K_f (mg/g)	n	R^2
SAHs H_3 in dry state	CV	231	277	4.2	0.99	37.15	2.53	0.96
	MB	270	294	9.5	0.99	64.56	3.03	0.95
SAHs H_3 in swollen state	CV	240	285	4.8	0.99	40.73	2.63	0.98
	MB	278	303	11.82	0.99	70.79	3.12	0.91

The thermodynamic equilibrium constant of Langmuir equation can be expressed in terms of enthalpy change (ΔH°) of adsorption process as a function of temperature. Assuming that, if standard enthalpy change (ΔH°) for the reaction is approximately independent of temperature, then slope of the linear plot of ln K_e vs. $1/T$ will be equal to $-\Delta H^\circ/R$. Now, the standard adsorption entropy change is determined from the equation as follows,

$$\Delta S^\circ = (\Delta H^\circ - \Delta G^\circ)/T \quad (11)$$

The plots of ln K_e vs. $1/T$ are represented in Fig. 8. Changes in ΔS° and ΔG° are used to determine whether the process is spontaneous or not. The negative Gibbs free energy change reveals the spontaneous nature of the adsorption process and its higher negative value indicates more energetically favorable adsorption [36]. The values of various parameters are summarized in Table 4.

It can be clearly observed from the Table 4 that the obtained values for standard enthalpy change are negative, thus suggesting that the adsorptions of both dyes are exothermic, which is also evidenced by the decrement in the adsorption of both dyes with increase in the temperature. Negative change in ΔG° values shows that the adsorption process is spontaneous [37] as well as, with the increase in temperature the decrease in the ΔG° values indicates the more spontaneous nature of the adsorption reaction at higher temperatures. The obtained positive value for entropy change shows increase in randomness at the solid-solution interface during the dye adsorption on the adsorbent.

3.11. Competitive adsorption of both dyes

The wastewater released from textile industries contains multiple pollutants. Therefore, it is desirable to investigate the adsorption of more than one pollutant from the aqueous solution. Thus, the adsorption of CV and MB dyes from their aqueous mixture was carried out and shown in Fig. 9. To investigate the competitive adsorption, SAHs sample were used in its dry as well as swollen condition. The concentration of both dyes was same in mixture (mg/L). In case of competitive adsorption three types of responses can take place: (i) the influence of mixture is more than that of each of the individual influence of the constituents present in the mixture (synergism); (ii) the influence of mixture is lesser than that of each of the individual influence of the constituents present in the mixture (antagonism); and (iii) the influence of mixture is not greater or lesser than that of each of the individual influence of the constituents present in the mixture (non-interaction) [38]. Adsorption of the CV/MB dye from the mixtures takes place in a similar manner as occur from the individual solution of each dye. It is worth mentioning that the adsorption capacity of poly(AAc-SA-AM)/SH SAHs for the adsorption of both dye was lower than the individual solution (antagonistic effect). The most logical reason for this type of action is claimed to be due to competition for the binding sites on the SAHs and/or a screening effect by the other dye molecules.

3.12. Desorption/regeneration of adsorbent

A good adsorbent in addition to its excellent adsorption ability should also exhibit good regeneration properties for multiple applications. The recovery of dyes is an important parameter for the characterization of economics of the process. Desorption studies helps in recovering the CV and MB dyes from the adsorbent surface and regenerating the SAHs, and thus it can be used again and again. Dyes desorption were also investigated in a batch experimental setup. The same SAHs poly(AAc-SA-AM)/SH which were

Table 4
Thermodynamic parameters for adsorption of CV and MB dye onto SAHs H_3 at various temperatures

		SAHs H_3 in dry state				SAHs H_3 in swollen state			
Dye	T (K)	$K_e \times 10^2$	ΔG° (kJ/mol)	ΔH° (kJ/mol)	ΔS° (J/mol K)	$K_e \times 10^3$ (kJ/mol)	ΔG° (kJ/mol)	ΔH° (kJ/mol)	ΔS° (J/mol K)
CV	303.15	4.20	3.61		7.80	4.80	3.93		4.75
	318.15	4.09	3.79	−1.24	8.00	4.52	4.12	−2.49	5.10
	333.15	4.01	3.97		8.19	4.34	4.32		5.49
MB	303.15	9.50	5.67		11.40	11.82	6.20		12.79
	318.15	9.11	5.95	−2.21	11.70	11.24	6.50	−2.32	13.13
	333.15	8.75	6.23		12.06	10.80	6.81		13.47

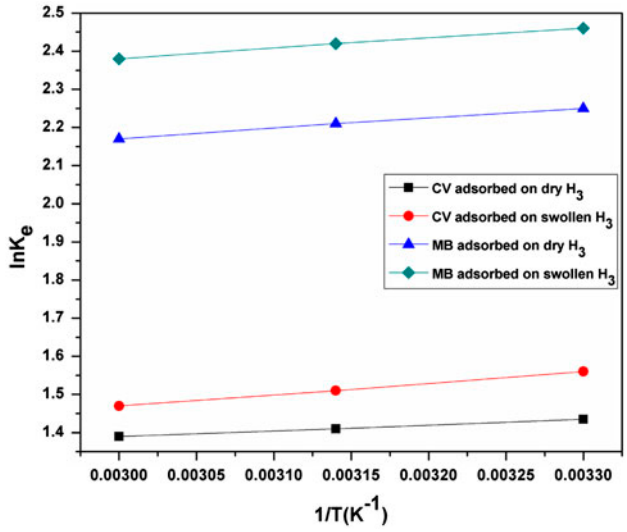

Fig. 8. Plot of ln K_e vs. T^{-1} for the evaluation of thermodynamic parameters of the phosphate ion adsorption process.

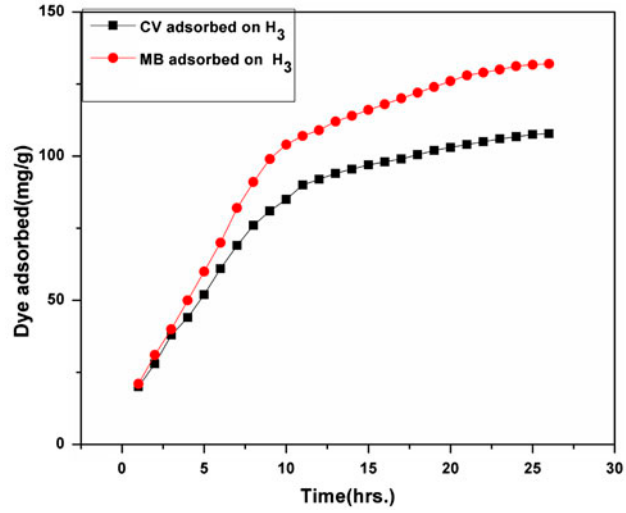

Fig. 9. Competitive adsorption of CV and MB dyes from their aqueous mixture.

applied for dye adsorption were placed in distilled water for 48 h and the amount of CV/MB dye desorbed to the distilled water was measured. Table 5 displayed the relationship between the adsorption amount and times for reuse for the SAHs sample. So after many times of reuse, the adsorption capacity of SAHs decreases only slightly as compared to initial capacity. It can be concluded that the SAHs poly (AAc-SA-AM)/SH showed stable CV/MB dye removal capacities after repeated regeneration.

Table 5
Adsorption amount of CV and MB dye onto SAHs H_3 after repeated adsorption–desorption cycle

	CV dye		MB dye	
Cycle no.	A	D	A	D
1	231.00	97.00	278.00	97.20
2	230.20	96.12	275.00	96.88
3	228.00	95.00	274.64	95.04
4	227.40	94.78	272.33	94.62
5	224.50	94.17	272.00	94.00

Note: A-adsorption (mg/g), D-desorption (%).

4. Conclusion

The study showed that both dyes CV and MB dye were removed effectively in high quantity from aqueous solutions using adsorbent poly(AAc-SA-AM)/SH SAHs in its dry as well as swollen state. Adsorption experiments were carried out at various conditions including time, SH content, temperature, and initial concentration of dye to investigate the optimized values of given parameters. The results revealed that poly(AAc-SA-AM)/SH SAHs adsorbs both dyes in higher amount with higher adsorption rate in its swollen condition as compared to dry state and the maximum adsorption amount was obtained when 2.4 wt.% SH content was used. The adsorption isotherms for CV and MB both dyes in its dry as well as swollen state agree well with the Langmuir adsorption isotherm model. The adsorption process of CV and MB dye onto poly(AAc-SA-AM)/SH SAHs is exothermic and spontaneous with the pseudo-second-order kinetics. The results of five time consecutive adsorption–desorption cycle show that the poly (AAc-SA-AM)/SH hydrogel has high reusability efficiency, indicating that it can be used as effective solid adsorbent for the removal of dye from waste water and aqueous effluents.

Acknowledgment

This work was financially supported by the University Grant Commission New Delhi, India (39-875-2010).

References

[1] K. Ravikumar, B. Deebika, K. Balu, Decolourization of aqueous dye solutions by a novel adsorbent: Application of statistical designs and surface plots for the optimization and regression analysis, J. Hazard. Mater. 122 (2005) 75–83.
[2] P. Dutta, An overview of textile pollution and its remedy, Indian J. Environ. Prot. 14 (1994) 443–446.

[3] K. Chen, J. Wu, C. Huang, Y. Liang, S.C. Hwang, Decolorization of azo dye using PVA-immobilized microorganisms, J. Biotechnol. 101 (2003) 241–252.
[4] Renmin Gong, Yi Ding, Utilization of powdered peanut hull as biosorbent for removal of anionic dyes from aqueous solution, Dyes Pigm. 64(3) (2005) 187–192.
[5] A. Alinsafi, M. Khemis, M.N. Pons, J.P. Leclerc, A. Yaacoubi, A. Benhammou, A. Nejmeddine, Electrocoagulation of reactive textile dyes and textile wastewater, Chem. Eng. Process. 44 (2005) 461–470.
[6] K. Swaminathan, S. Sandhya, A. Sophia Carmalin, K. Pachhade, Y.V. Subrahmanyam, Decolorization and degradation of H-acid and other dyes using ferrous–hydrogen peroxide system, Chemosphere 50 (2003) 619–625.
[7] M. Muthukumar, N. Selvakumar, Studies on the effect of inorganic salts on decolouration of acid dye effluents by ozonation, Dyes Pigm. 62 (2004) 221–228.
[8] G. Ciardelli, L. Corsi, M. Marucci, Membrane separation for wastewater reuse in the textile industry, Resour. Conserv. Recycl. 31 (2000) 189–197.
[9] T. Panswed, S. Wongchaisuwan, Mechanism of dye wastewater color removal by magnesium carbonate-hydrated basic, Water Sci. Technol. 18 (1986) 139–144.
[10] I.D. Mall, V.C. Srivastava, N.K. Agarwal, I.M. Mishra, Removal of congo red from aqueous solution by bagasse fly ash and activated carbon: Kinetic study and equilibrium isotherm analyses, Chemosphere 61 (2005) 492–501.
[11] M. Mitchell, W.R. Ernst, G.R. Lightsey, Adsorption of textile dyes by activated carbon produced from agricultural, municipal and industrial-wastes, Environ. Contam. Toxicol. 19 (1978) 307–311.
[12] K. Kosemund, H. Schlatter, J.L. Ochsenhirt, E.L. Krause, D.S. Marsman, G.N. Erasala, Safety evaluation of superabsorbent baby diapers, Regul. Toxic. Pharmac 53 (2009) 81–89.
[13] L.C. Dong, A.S. Hoffman, A novel approach for preparation of pH-sensitive hydrogels for enteric drug delivery, J. Controlled Release 15 (1991) 141–152.
[14] S.K. Bajpai, S. Singh, Analysis of swelling behavior of poly(methacrylamide-co-methacrylic acid) hydrogels and effect of synthesis conditions on water uptake, React. Funct. Polym. 66 (2006) 431–440.
[15] E. Karadag, D. Saraydin, Y. Caldiran, O. Guven, Swelling studies of copolymeric acrylamide/crotonic acid hydrogels as carriers for agricultural uses, Polym. Advance Technol. 11 (2000) 59–68.
[16] C.O. Walker, U.S. Patent 4: 664, 1987.
[17] A.T. Paulino, M.R. Guilherme, A.V. Reis, G.M. Campese, E.C. Muniz, J.J. Nozaki, Removal of methylene blue dye from an aqueous media using superabsorbent hydrogel supported on modified polysaccharide, J. Colloid Interface Sci. 301 (2006) 55–62.
[18] V. Bekiari, M. Sotiropoulou, G. Bokias, P. Lianos, Use of poly(N,N-dimethylacrylamide-co-sodium acrylate) hydrogel to extract cationic dyes and metals from water, Colloids Surf. A 312 (2008) 214–218.
[19] E.K. Yetimoglu, M.V. Kahraman, O. Ercan, Z.S. Akdemir, N.K. Apohan, N-vinylpyrrolidone/acrylic acid/2-acrylamido-2-methylpropane sulfonic acid based hydrogels: Synthesis, characterization and their application in the removal of heavy metals, React. Funct. Polym. 67 (2007) 451–460.
[20] W. Wang, A. Wang, Synthesis, swelling behaviors, and slow-release characteristics of a guar gum-g-poly (sodium acrylate)/sodium humate superabsorbent, J. Appl. Polym. Sci. 112 (2009) 2102–2111.
[21] J. Hizal, R. Apak, Modeling of cadmium(II) adsorption on kaolinite-based clays in the absence and presence of humic acid, Appl. Clay Sci. 32 (2006) 232–244.
[22] D.S. Olpan, S. Duran, D Saraydin, Adsorption of methyl violet in aqueous solutions by poly(acrylamide-co-acrylic acid) hydrogels, Rad. Phys. Chem 66 (2003) 117–225.
[23] Y. Wang, Li. Zeng, X. Ren, H. Song, A. Wang, Removal of Methyl Violet from aqueous solutions using poly(acrylic acid-co-acrylamide)/attapulgite composite, J. Environ. Sci. 22 (2010) 7–14.
[24] S. Hua, A. Wang, Synthesis, characterization and swelling behaviors of sodium alginate-g-poly(acrylic acid)/sodium humate superabsorbent, Carbohydr. Polym. 75 (2009) 79–84.
[25] J. Liu, Q. Wang, A. Wang, Synthesis and characterization of chitosan-g-poly(acrylic acid)/sodium humate superabsorbent, Carbohydr. Polym. 70 (2007) 166–173.
[26] E. Karadag, D. Saraydin, O. Guven, Use of superswelling acrylamide/maleic acid hydrogels for monovalent cationic dye adsorption, Sep. Sci. Technol. 30 (1995) 3747–3760.
[27] E. Karadag, D. Saraydin, O. Guven, Behaviors of acrylamide itaconic acid hydrogels in uptake of uranyl ions from aqueous solutions, Sep. Sci. Technol. 30 (1995) 3287–3298.
[28] S. Lagergren, K.S. Vetenskapsakademiens, About the theory of so called adsorption of soluble substances, Handlingar 24 (1898) 1–39.
[29] Y.S. Ho, G. McKay, Pseudo-second order model for sorption processes, Process Biochem. 34 (1999) 451–465.
[30] V.C. Srivastava, M.M. Swamy, I.D. Mall, B. Prasad, I.M. Mishra, Adsorptive removal of phenol by bagasse fly ash and activated carbon: Equilibrium, kinetics and thermodynamics, Colloids. Surf. A 272 (2006) 89–104.
[31] I.J. Langmuir, The adsorption of gases on plane surfaces of glass, mica and platinum, J. Am. Chem. Soc. 40 (1918) 1361–1403.
[32] Y.S. Ho, C.T. Huang, H.W. Huang, Equilibrium sorption isotherm for metal ions on tree fern, Process Biochem. 37 (2002) 1421–1430.
[33] M. Jaroniec, Physical adsorption on heterogeneous solids, Adv. Colloid Interface Sci. 18 (1983) 149–225.
[34] Y. Liu, Some consideration on the Langmuir isotherm equation, Colloids. Surf., A 274 (2006) 34–36.
[35] M. Alkan, O. Demirbas, S. Celikcapa, M. Dogan, Sorption of acid red 57 from aqueous solution onto sepiolite, J. Hazard. Mater. 116 (2004) 135–145.
[36] K.S. Walton, J. Cavalcante, M.D. LeVan, Adsorption of light alkanes on coconut nanoporous activated carbon braz, J. Chem. Eng. 23 (2006) 551–561.
[37] J.M. Smith, H.C. Van Ness, Introduction to Chemical Engineering Thermodynamics, 4th ed., McGraw-Hill, New York, NY, 1987.
[38] Y. Sag, Biosorption of heavy metals by fungal biomass and modeling of fungal biosorption: a review, Sep. and Puri. Meth. 30(1) (2001) 1–48.